17th World Conference on Earthquake Engineering, 17WCEE
Sendai, Japan - September 13th to 18th 2020

SEISMOTECTONIC PROSPECTIVE ADJACENT TO MAIN FRONTAL THRUST AND GANGA FOREDEEP IN THE GARHWAL HIMALAYA, INDIA

Arup.Sen[(1)], S.C.Gupta[(2)], M.L.Sharma[(3)], A.Kumar[(4)]

[(1)]*Fellow, Dept. of Earthquake Engineering, IIT Roorkee, sarup_iit@yahoo.co.in*
[(2)]*Associate Professor, Dept. of Earthquake Engineering, IIT Roorkee, scgeqfeq@iitr.ac.in*
[(3)]*Professor, Dept. of Earthquake Engineering, IIT Roorkee, mukutfeq@iitr.ac.in*
[(4)]*Formerly Professor, Dept. of Earthquake Engineering, IIT Roorkee, ashwnfeq@iitr.ac.in*

Abstract

Piedmont fault (PF) mapped to the south of the Main Frontal thrust (MFT) is tectonic uplifts which is assumed to represent an emerging new plate boundary below the Indo-Gangetic Plains (IGP). In this study we elucidate the geometry of the PF and the MFT from the attributes of local seismicity, fault plane solutions, and space-depth distribution of events from 265 well located local earthquakes, and interpret the seismotectonics beneath the IGP and the segment of the MFT, that marks the southern boundary of the Garhwal Sub-Himalaya (GSH).

The fault plane solutions of 69 local events obtained using P-wave polarity and body wave amplitude ratios, reveals mixture of thrust, normal and strike–slip faulting in the above tectonic domains. Events adjacent to the MFT and the PF occur at very shallow depths, and show normal faulting whereas, most of the events in the IGP, that occur at the extreme southern end of the MFT, show thrust faulting. Further, the events having normal faulting with some strike-slip components show arc-normal (NE-SW) and arc parallel (NW-SE) extensions in different parts of IGP. Events associated with normal faulting are attributed to the lithospheric flexing because of northward push of the Indian plate and subsequent forming of peripheral fore-deep. The inversion results of FPSs of 69 events suggest a dominant reverse faulting with a strike slip component on a preferred north dipping plane. The N45°E oriented maximum principal stress with 12° plunge corroborates well with the northward movement of the Indian plate. The depth wise stress inversion results also show that the direction of compressive stress is near north-northeast—south-southwest in IGP.

Space-depth distribution of seismicity reveals that the depth of the upper surface of the Indian plate in the IGP is about 8-10 km. In the vicinity of MFT, the events occur at shallow depths as well as at deeper level. Activity at shallow depths appears to be associated with the Piedmont fault zone, whereas the activity at deeper level defines a seismogenic source zone at depth, between 10 to 30 km. This seismogenic source zone lies much below the plane of detachment. It is conspicuous to note that trend of seismic activity from southwest to northeast direction defines a major tectonic feature beneath the IGP which seems to continue from a depth of about 10 km to a depth of at least 30 km. The linear dimension of this feature is about 80 km. From this study it appears that, the stress is accumulating in the lower crust of the Indian plate at a depth between 10 and 30 km in the IGP. From the distribution of seismic activity below the MBT it appears that the thickness of the seismogenic crust is about 30 km.

Keywords: Piedmont fault, Main Frontal thrust, Indo-Gangetic Plains and Garhwal Sub-Himalaya.

1. Introduction

The Himalaya has been formed by the continental- continental convergence of Indian plate with the Eurasian plate. Due to this continental collision the Himalayan region is divided from south to north into three sub-regions, the Sub Himalaya (SH), the Lesser Himalaya (LH) and the Higher Himalaya (HH) which are separated by the Main Boundary Thrust (MBT) in the south and the Main Central Thrust (MCT) in the north. Further south of the Sub Himalaya the region is disignated as the Ganga fore-deep basin or Indo-Gangetic Plains (IGP) which is separated from the Sub Himalaya by Main Frontal thrust (MFT) (**Fig. 1**). Almost east-west trending elongated Ganga basin, also called Himalayan fore-deep, forms the part of IGP also showed the impression of Piedmont fault (PF).

The focus of the present study is to understand the seismotectonics of the region around IGP and the Sub Himalaya with particular emphasis on the seismicity of the segment of Main Frontal Thrust (MFT). The study is based on the local eartquake data that has been analyzed and interpreted to study mechanics of the faulting, stress orientations, and space-time distributions of seismicity.

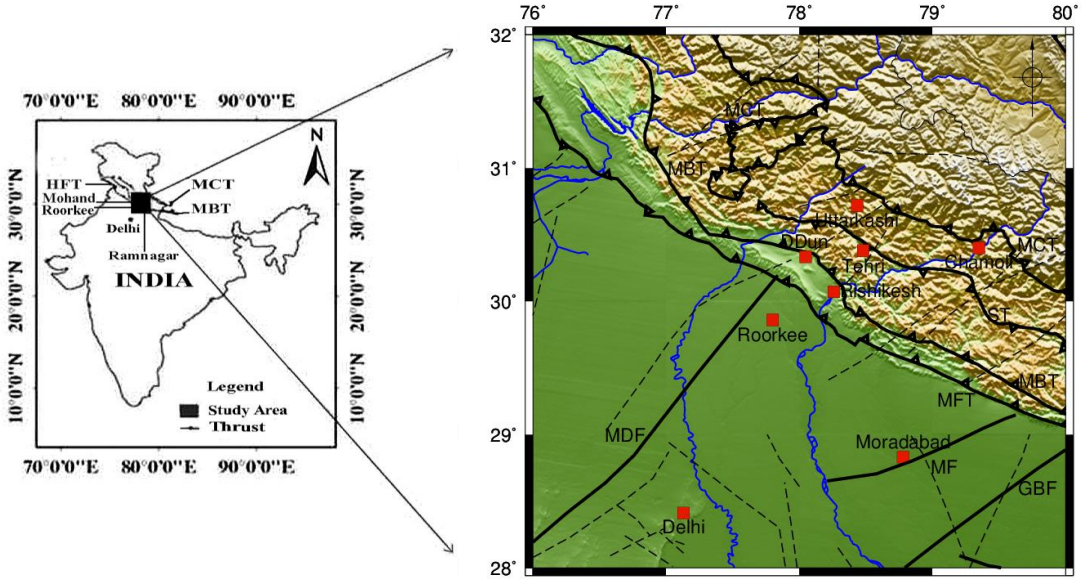

Fig. 1- Map showing the study area along with various tectonic features and towns (Tectonics after GSI, 2000 map).

The study area is bound between latitude 29.0° to 30.50° N and longitude 76.00° to 80.00° E (**Fig.1**). Major parts of the study area fall in the Garhwal Himalaya in the state of Uttarakhand and encompasses three distinct tectonic domains---the Indo-Gangetic Plains (IGP), the Garhwal Sub Himalaya (GSH) and the Garhwal Lesser Himalaya (GLH). The major rivers of the region around the study area are Ganga and Yamuna. The study area is flanked to the east by Moradabad fault and to the west by Delhi–Hardwar Ridge (DHR). The broad geologic and tectonic framework of the study area is shown in **Fig 1**.

2. Data sets used in the study

The local earthquake data used in the study are recorded through the operation of two networks. The first data set consist of 35 local events occurred in the study area from 1995-2007 collected through the operation of 6-station local network. The second data set comprises 230 local events occurred in the region during 2008-2018 and recorded by a 12- station local network deployed around Tehri region in the GLH since 2008. Triaxial-short-period-seismometer (CMG 40T-1, frequency range 1-100 Hz.), 24-bit digitizer and data acquisition system (DAS 130-01/03) records the digital data. The three component digital data is acquired at a 100 samples/sec (Sharma, et al., 2016). Data of one independent station Roorkee (RKE) at IGP has been

also used. These data sets are used to estimate hypocenter parameters of local events. The hypocenter parameters of 35 and 230 local events were estimated employing Hypo71PC computer program and HYPOCENTER program (Lienert and Havskov, 1995) respectively using velocity model given by Kumar et al. (1994). Only those events having standard errors in origin time (RMS) ≤ 0.50 sec, latitude and longitude (ERH) ≤ 5.0 km and focal depth (ERZ) ≤ 5.0 km have been considered for analysis. **Fig 2** shows the distribution of epicenters of 265 events.

3. Pattern of local seismicity

Spatial distribution of local seismicity based on the locations of the 265 events is depicted in the **Fig. 2**. The distribution of 35 events belonging to first data set is shown by filled blue asterisks. It is seen that only 9 events are located to the southwest of the MFT and in the IGP. Out of these 9 events 4 events are located in the close proximity of the MFT and remaining 5 are located much away from the MFT in the IGP. It is interesting to note that the epicenters of 4 events define a northwest–southeast trend. 10 events are located in the GSH between the MFT and the MBT. Out of the remaining 16 events, 13 events are located in GLH between the MBT and the Srinagar thrust.

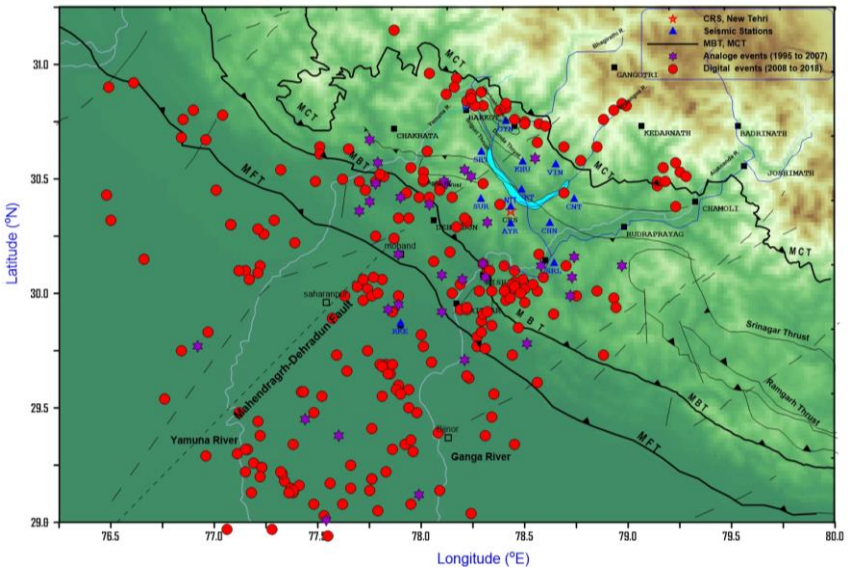

Fig. 2- Epicenters of earthquakes recorded in the study area along with tectonic features.

The locations of 230 events belonging to the second data set are shown in the **Fig. 2** by red solid circles. Out of these 230 events, 108 events are located in the IGP and 6 events coincide with the trend of MFT, 33 events located in GSH and remaining 83 events are located in the GLH and in the close proximity of the MCT including 10 events that are located in the Garhwal Higher Himalaya (GHH). Out of 108 events located to the southwest of the MFT, 28 events follows the trend of new emerging fault boundary called Piedmont fault (PF) occur in the IGP.

The distribution patterns of local events have brought out one well defined cluster of activity, the center of which is located about 10 km northwest of Roorkee. This cluster falls 20 km southwest of the surface trace the MFT and is almost located at the northeast end of the Mahendragarh-Dehradun Sub-Surface Fault (MMDS) (**Figs. 1** & **2**). Part of the seismic activity, defining a northwest to southeast trend, occurs at a distance of about 20 km south of Roorkee. Several local events occur at a distance of about 100 km southwest of Roorkee. These events are distributed over a wider area and activity seems to terminate to the east of the Yamuna river. One of the conspicuous feature of the observed distribution of the seismic activity is that about 85% of activity occur right side of the Mahendragarh-Dehradun Sub-Surface Fault (MDSSF) between MDSSF and the Ganga river. Only 15% of the events are located in the region falling northwest of the MDSSF.

4. Determination of Fault Plane Solutions

The physical process of elastic strain accumulation and the triggering mechanism are the basics to understand the earthquake kinematics. In this context, FPS describes the geometry and mechanism of the faulting during an earthquake. FPSs of 69 best conceive events falls in the Sub-Himalaya and IGP are estimated from amplitudes and polarities of the vertical P- wave motion are interpreted. The FPSs are deduced from first motion direction of P- wave of more than eight stations. In order to compute FPS, computer program FOCMEC_EXE (Snoke et al., 1984) has been used. This program forms part of the SEISAN program. The Input data for the program are polarities and amplitude ratios of direct waves of the same type (i.e., Pg and Sg). The FPSs are obtained from polarities while the amplitude ratios are used to constrain the solutions. It is observed that events falling to the southwest of Roorkee have fewer solutions because of the poor station configuration. The numbers of polarity errors are selected depending on the available data values and the value of 2 is selected from the recommended range of 0 to 5. For maximum amplitude ratio error, value of 0.1 is selected. This ratio means that errors are within 10%. Based on the input data the program makes an efficient and systematic grid search for focal sphere based on defined criteria of acceptable number of wrong polarities and amplitude ratio errors.

Fig. 3 depicts FPSs along with locations of local events. FPSs show all types of solutions i.e., strike-slip, reverse and normal faulting and it is seen that events located very close to each other have different mechanisms. Since rupture length of local events (M>3) are of the order of few hundred meters to about one km and events may occurs on faults with different orientations. From total 69 events, 29 events show normal faulting and with the component of normal left-lateral and pure dip slip. 32 events show reverse faulting and reverse faulting with left-lateral component while 8 events show left lateral strike slip mechanism.

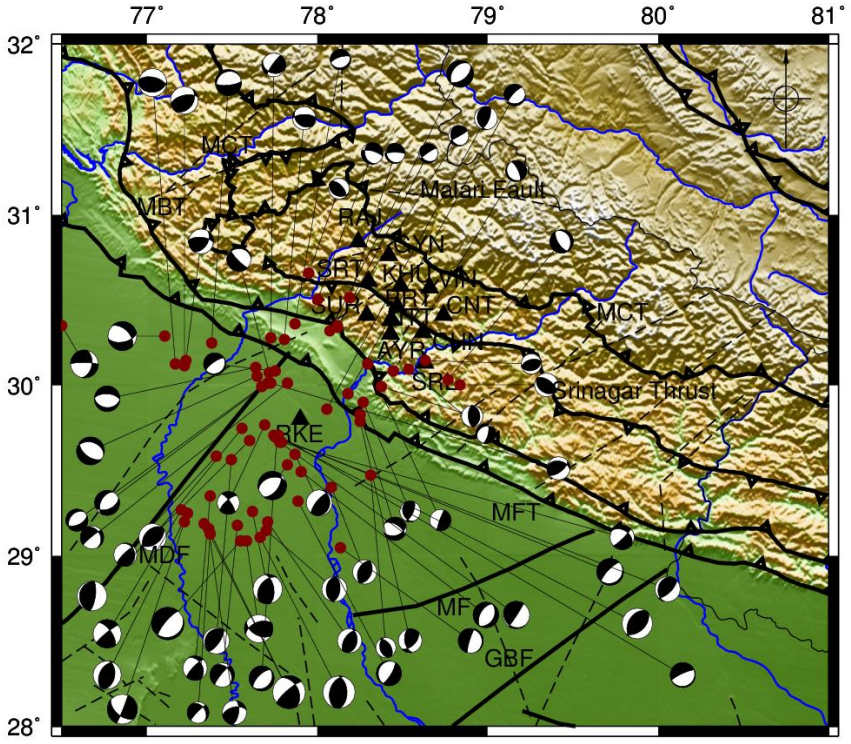

Fig. 3- Focal mechanism solutions of well-located earthquakes deduced from P-wave polarity and amplitude ratios presented by 'beachball' diagrams along with the tectonic features of the study area.

A cluster of events, located about 20 km northwest of Roorkee station show normal faulting with pure dip slip and left lateral components. Most of the events straddling the traces of MFT and pediment fault indicate normal faulting. A number of events aligned in the northeast-southwest direction show reverse faulting and few events follow the trend of Ganga River upto Sirala station (SRL) show reverse faulting. 8 events display pure strike slip faulting. Most of these events occur in the south of IGP at the focal depth range from 15 to 30 km. The events confined to the depth range between 31 and 40 km occur to the south of the MFT. Most of the lower focal depth events occur and span in the vicinity of foot-hills zone and the upper part of IGP located close to MFT are seems to be related to Piedmont fault (PF).

5. Stress Tensor Inversion using Focal Mechanism Estimates

To allow estimating the principal-stress orientations from FPSs of different clusters, focal mechanism stress tensor inversion (FMSI) program proposed by Gephart's (1990) ---an extension of the algorithm proposed by Gephart and Forsyth (1984), is used in the study. This program finds out the best fitting orientation of principal stress tensor to a number of earthquakes by grid search technique over a range of possible models assuming that the slip on the fault planes occur in the direction of the resolved shear stress. This method provides stress models that are most reliable for a given set of FPSs.

The best fitting stress tensor parameters obtained includes the azimuths and plunges of the three principal stresses and R---a measure of stress magnitude. R, indicates the magnitude ratio of the intermediate principal stress relative to the two extreme ones and given as $R=\sigma_2-\sigma_1/\sigma_3-\sigma_1$ where σ_1=S1, σ_2=S2 and σ_3=S3 are the greatest, intermediate and least principal stresses respectively. The position of maximum principal axis closest to vertical indicates dominant Normal faulting stress regime, minimum stress axis near vertical shows reverse faulting stress regime and intermediate stress axis nearest to vertical indicates strike-slip faulting stress regime. The oblique attitude of minimum and intermediate stress axes highlights the association of reverse and strike-slip faulting types.

Above method is applied to FPSs of 69 local events and their different groups, which scattered in the part of Ganga Fore deep and the IGP to understand the broad deformation characteristics of probable faults or fractures associated with the different clusters of local events. The data set of 69 events is divided in to five different groups/clusters according to their occurrence in different parts of the studied area. The cluster 1 is most important as it follows the trend of the MFT. Clusters 2, 3 and 4 fall to the south of the Roorkee station, whereas cluster 5 follows the trend of Ganga River. The clusters of the local events selected for stress tensor analysis are shown in **Fig. 4** and results are tabulated in **Table 1**.

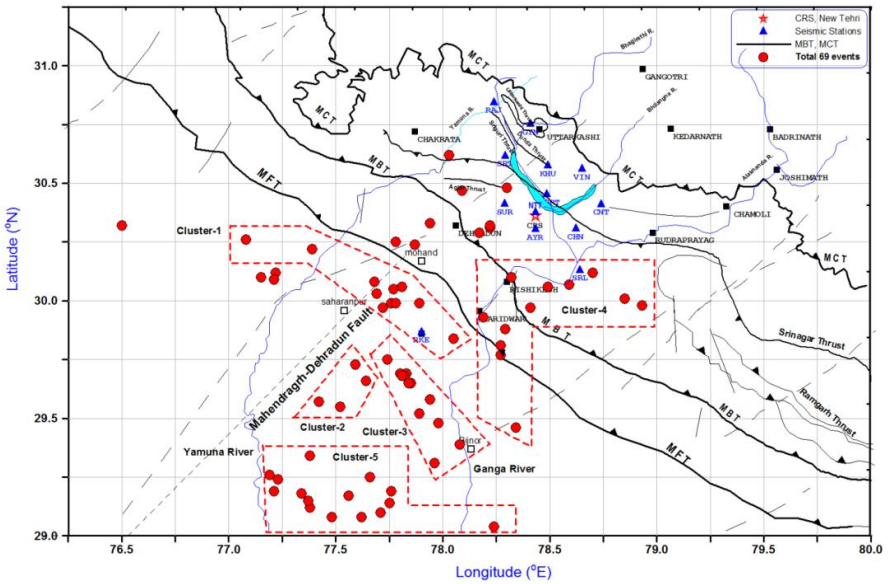

Fig.4 - Clusters of events used for the focal mechanism stress tensor inversions.

Table 1. Stress tensor inversion results of the total events and its five clusters. This includes azimuth and plunge of the principal stress axes and values of R, M and stress regime of five clusters.

Cluster	σ 1		σ 2		σ 3		Stress Mag.(R)	Misfit F (Degree)	Faulting style of Stress regime
Dataset	Trend (Azm.)	Plunge	Trend (Azm.)	Plunge	Trend (Azm.)	Plunge			
Total	45^0	12^0	135^0	2^0	232^0	78^0	0.5	13	Thrust
Cluster 1	63^0	62^0	324^0	5^0	232^0	27^0	0.5	4.2	Normal
Cluster 2	247^0	5^0	338^0	9^0	129^0	80^0	0.6	0.9	Thrust
Cluster 3	134^0	11^0	348^0	77^0	225^0	7^0	0.4	8.4	Strike slip
Cluster 4	157^0	2^0	66^0	36^0	250^0	54^0	0.3	11	Thrust
Cluster 5	41^0	8^0	142^0	52^0	305^0	36^0	0.1	4.9	Strike slip

This scheme is applied to the FPSs of all 69 events. The results were calculated at the 95% confidence limit. Further the greatest and least principal stress components do not overlap with each other. The inversion results show thrust faulting with average misfit of 13^0 and values of stress magnitude (R) = 0.5 which shows maximum principal stress axis (σ_1) trending 45^0 with 12^0 plunge, intermediate principal stress ($\sigma 2$) trending 135^0 with 2^0 plunge and least principal stress (σ_3) trending 232^0 with 78^0 plunge respectively. The large misfit of the order of 13^0 suggests a relatively more heterogeneous stress regime for total events (Gillard et al., 1992). However, the N45°E orientation of maximum principal stress with 12^0 plunge corroborates well with the prevailing north-south and south-west orientation of the regional compression resulted from the northward movement of the Indian plate. **Fig. 5a** depicts the stress tensor inversion result of total events.

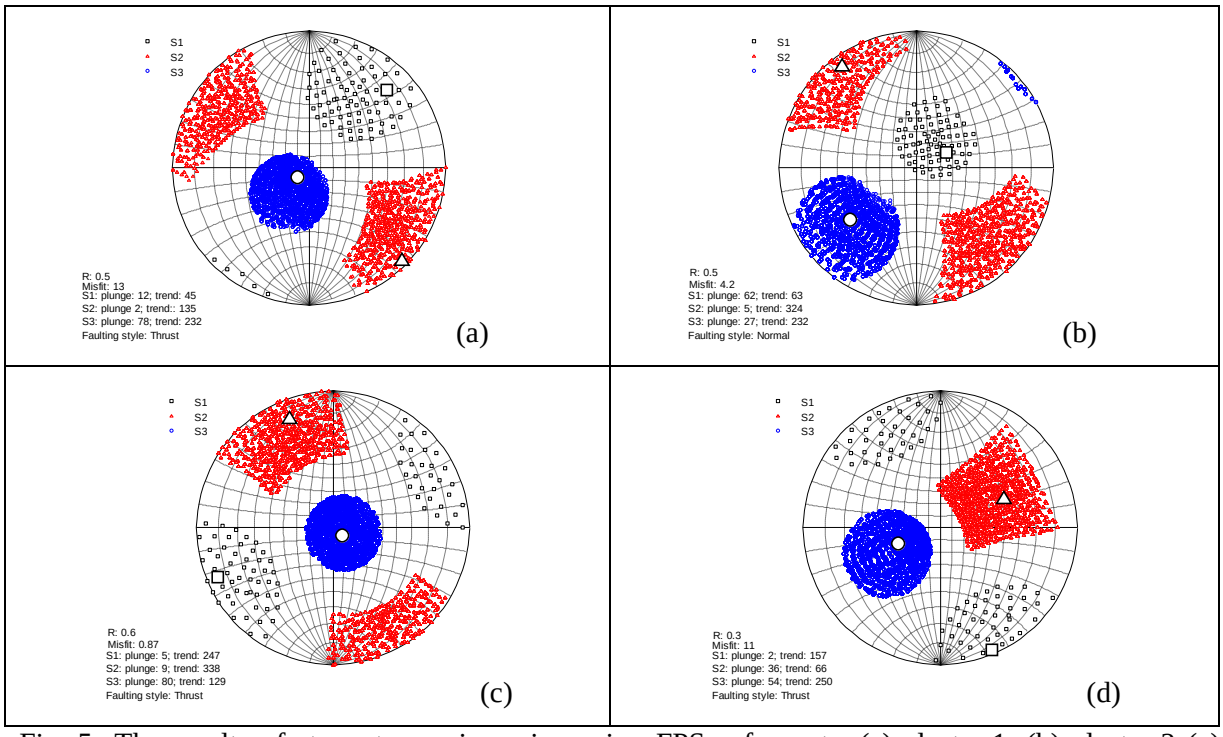

Fig. 5- The results of stress tensor inversion using FPSs of events. (a) cluster-1, (b) cluster-2 (c) cluster-3 and (c) cluster-4. Black (σ1), Red (σ2) and Blue (σ3) symbol shows 95% confidence region where greatest (□-S1), intermediate (Δ-S2) and least (0-S3) indicates principal stress respectively.

Application of stress tensor inversion to the FPSs of cluster 1 showed average misfit of 4.2^0 and values of stress magnitude (R) = 0.5 with normal faulting. Results indicated within 95% confidence limit and the greatest and least principal stress components do not overlap. The maximum principal stress axis (σ_1) trends 63^0 with 62^0 plunge, the intermediate principal stress (σ_2) trends 324^0 with 5^0 plunge and the least principal

stress (σ_3) trends 232^0 with 27^0 plunge. The small misfit value of 4.2^0 suggests a relatively homogeneous stress regime and east of northeast direction of principal stress axes. Events belonging to cluster-1 fall to the south and trend parallel to MFT. It appears that this region of fore-deep is undergoing stretching with steep plunge of 62^0 shows normal faulting (**Fig. 5b**). The cluster-2 comprises 4 events and the inversion result shows, thrust/reverse faulting. The average misfit of 0.87^0 and value of stress magnitude R= 0.6 are estimated. The σ_1 trends 247^0 with 5^0 plunge, σ_2 trends 338^0 with 9^0 plunge and σ_3 trends 129^0 with 80^0 plunge. The small misfit value 0.87^0 suggests a relatively homogeneous stress regime with west-southwest direction of principal stress regime (**Fig. 5c**). For cluster-3, the inversion of FPSs show thrust/reverse faulting. The results show average misfit of 11^0 and value of stress magnitude, R= 0.3. The σ_1 trends 157^0 with very shallow plunge of 2^0, σ_2 trends 66^0 with 36^0 plunge and least σ_3 trends 250^0 with 54^0 plunge. The misfit value of 11^0 suggests a relatively heterogeneous stress regime with south-southeast direction of principal stress regime (**Fig. 5d**). The inverted FPSs for cluster-4, shows strike slip mechanism with average misfit of 8.4^0 and values of stress magnitude R= 0.4. The σ_1 trends 134^0 with 11^0 plunge, σ_2 trends 348^0 with 77^0 plunge and σ3 trends 225^0 with 7^0 plunge. A relatively heterogeneous stress regime is inferred from the misfit value of 8.4^0. The principal stress regime has southeast direction. The inversion result for cluster-5, shows, strike slip mechanism. The average misfit of 4.9^0 and values of stress magnitude R= 0.1 are estimated. The σ_1 trends 41^0 with 8^0 plunge, σ_2 trends 142^0 with 52^0 plunge, and σ3 trends 305^0 with 36^0 plunge. The moderate misfit value of 4.9^0 suggests a relatively homogeneous stress regime with northeast direction of principal stress regime.

6. Depth-wise Stress Tensor Analysis

Stress tensor inversion has been conducted for events occurring at different depth ranges using the FPS of 69 local events. As discussed earlier, from different FPSs, the orientation of stress tensor can be calculated assuming uniform stress field. The focal mechanisms of events in four depth ranges are inverted and results are represented in **Fig. 6**.

The inversion of focal mechanisms of events in the depth range of 0 to 11 km shows well constrained σ1 and σ3 with 95% confidence limit. An average misfit of 4.1^0, which is low and may be attributed to small number of FPSs used in inversion. The stress magnitude R = 0.1 with $N32^0$ azimuth and $N016^0$ plunge of σ1, $N228^0$ azimuth and $N73^0$ plunge of σ2; and $N123^0$ azimuth and $N04^0$ plunge of σ3. The principal compressive stress (σ1) is oriented in NNE-SSW direction. This is consistent with the ongoing direction of the India-Eurasia collision. The inversion of FPSs of events in the depth range 12 to 20 km provides relatively large uncertainty in the estimation of σ1 and σ3 with 95% confidence limits. The results show an average misfit of 11^0 and R = 0.9. The σ1 trends $N308^0$ with 38^0 plunge and σ3 trends $N168^0$ with 44^0 plunge. The σ1 (compressive stress) is oriented in the WNW-ESE direction. The large spread within 95% confidence limits for σ1 and σ3 indicates that the stress field is not homogeneous, possibly because of several local fractures and faults in the Sub Himalaya and IGP. The presence of transverse fault and lineaments, in and around the study area are also proposed by Sharma & Lindholm, (2012).

The inversion of FPSs of event in the depth range from 21 to 31 km provided a relatively stable uncertainty of σ1 and σ3 within 95% confidence limit. The results show an average misfit of 11^0 and R = 0.3, and show strike slip faulting with σ1 trending $N11^0$ with 07^0 plunge and σ3 trending $N104^0$ with 20^0 plunge. The orientation of σ1 in NS direction conforms to the direction of the India-Eurasia collision. The σ3 (tensional axis), showing almost parallel orientation in agreement with the strike direction of MFT and MBT.

The inversion of FPSs of events in the depth range from 32 to 40 km gave well constrained uncertainty of σ 1 and σ 3 within 95% confidence limit. The results show normal faulting with an average misfit of 09^0 and R = 0.5. The σ1 trends $N356^0$ with 56^0 plunge and σ3 trends $N259^0$ with 4^0 plunge. The azimuth of σ 1 is almost vertical i.e. in north-south direction. Well constrained limits of σ1 and σ3 and average misfit of 09^0 indicate that prevailing stress field is homogeneous in character. The σ1 directed almost is north-south which could be attributed to the flexing of Indian plate.

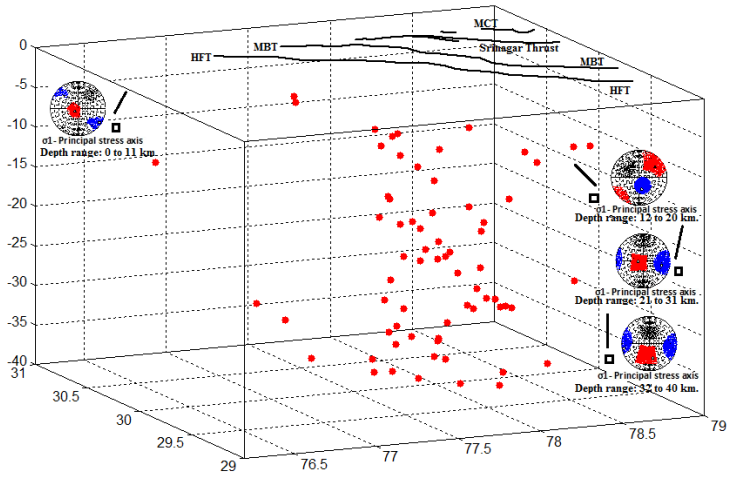

Fig. 6- 3-D depth wise plot of 69 events and their stress tensor inversion using FPSs. where symbol (□- S1) show greatest principal stress.

7. Depth sections and its seismotectonic prospective

A 270 km long depth section A-A' and 280 km long B-B', has been drawn from the IGP to the Higher Himalaya to infer the broad seismotectonic model of the study area. The 120 km wide traverse A-A' section cuts across the HFT, the MBT, the SNT and the MCT and 40 km wide cross section along the surface trace of MFT has been drawn. Focal depth distributions of 265 local events along with two cross-sections are depicted in **Fig. 7.1**. Over all entire study is based on the events, mostly falls in the region around Sub-Himalaya and Indo-Gangetic Plains (IGP) but few events following MCT and Higher Himalaya also considered to explain the whole depth–space cross section of Garhwal Himalaya.

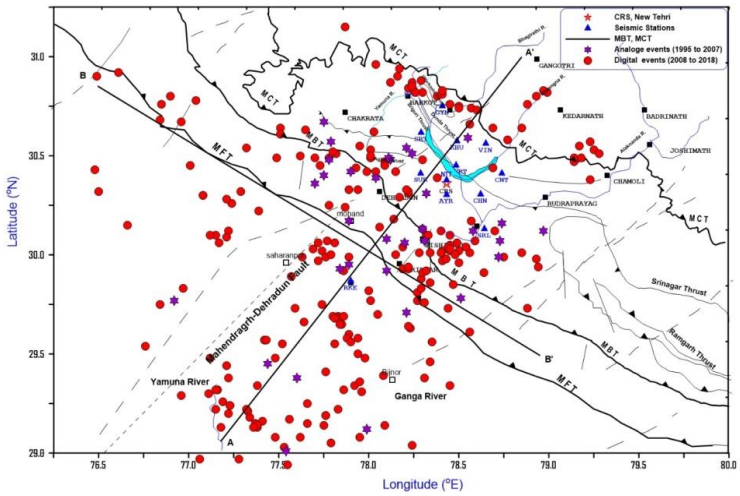

Fig. 7.1 Distribution of epicenters of events in the study area. A-A' shows the traverse along and B-B' across the prominrnt thrust upon which the depth cross section is drawn.

The focal depth distribution of A-A' section are shown in **Fig. 7.2**. From the pattern of space-depth distribution of seismicity, a seismogenic source has been delineated to the southwest of the MFT, at least up to the depth of 30 km. This source lies at a depth of 10 km and continues from the depth of 10 km to at least 30 km (from shallow to mid crustal depths) (Sen, 2016; Sen, et al., 2018). To the northeast of the section, the depth distribution of events in the vicinity of the MCT is shown in **Fig. 7.2**, and it is found that these events occur at shallow depths up to 15 km.

Depth distribution of seismic activity delineates two seismicity zones along the length of the traverse A-A'. First zone seems to represent the seismic activity of the upper surface of the detachment and second zone represent the seismicity of the upper crust of the under thrusting Indian plate. Based on the distribution of seismicity it appears that the depth of the upper surface of the Indian plate in the IGP (southwest of the MBT) is about 8-10 km which agrees with the depth estimates given by Khattri et al. (1989). The major difference between the present study and that of Khattri et al. (1989) is the focal depth of the events. Major seismic activity occurred in the vicinity of MCT up to the 15 km, and focal depths of the events found to increase from 15 km to about 40 km below the MBT and the SNT whereas, Khattri et al. (1989) has reported the focal depth of local earthquakes <10 km with very little activity observed at a depth between 10 and 20 km and no activity below 20 km depth in the Garhwal Himalaya. The locations of events at deeper level, in the present study, indicate the depth of the Moho discontinuity is at about 40-50 km.

Seismic activity at shallow depths in the vicinity of the HFT seems to overlap the Piedmont fault which clustered 20 km west of Roorkee in the northwest-southeast direction, with a gentle dip of 6^0 -7^0 due northeast and showing acute angle dip at NW direction. This trend is also ratified by Thakur (2013). Bhattacharya and Kayal (2005) postulated that source of 2005 Kangra earthquake lies south of MBT beneath the HFT. They argued that a seismogenic source zone lies at a depth of 30-40 km in the lower crust. Source of Dehradun earthquake (Ms~7) is also estimated at a depth of 30-40 km to the south of MBT (Hough et al., 2005). The depth of 30-40 km does not conform to the conceptual tectonic model that postulates occurrence of earthquakes on the plane of detachment. Further, the interpretation of local earthquakes data collected from the operation of local network have brought out a deeper seismogenic source zone (30-40 km) in the vicinity of MFT. This source zone lies much below the plane of detachment south of the MBT as proposed by Seeber et al. (1981). Kayal (2010) argued that MFT is the possible seismogenic thrust and along this thrust the tectonic stress is accumulated in the lower crust at a depth of 30-40 km and seems to be the cause of earthquakes. The local seismicity observed at deeper level (i.e., 30-40 km) in this study below the MBT, the SNT and the MFT follows with the argument given by Kayal (2010). In the recent study related to the seismicity around the IGP, Mahesh et al. (2015) reported the occurrence of nine events with focal depths between 25 to 45 km. The focal depths of the event observed in the present study conform to those reported by Mahesh et al. (2015).

Fifteen events occurred to the south of the HFT at a depth of about 10 km. Their location conforms to the location of Piedmont fault and almost every events are show normal faulting. In depths ranging from 30 km to 40 km twenty eight events occurred in the vicinity of the HFT and the Lesser Himalaya (between 110 km to 160 km). From southwest to northwest (from the beginning of the section) up to the distance of 60 km, the focal depths of events along the section gradually increases from 10 km to about 25 km. The events located between 70 km and 100 km along the section have focal depths from 30 to 40 km. These events also define an increasing trend in the focal depths with distance.

The presence of a major tectonic feature in the IGP indicated by the distribution of the local seismicity. The focal depths of events increase from 10 km to 30 km as we traverse from southwest to northeast. This shows a seismogenic feature with linear dimension of about 80 km. This hidden seismogenic feature beneath the IGP continues from upper crust to lower crust. The activity associated with this features is very different from the upper surface detachment plane.

Depth distribution of hypocenters along the section A-A' from southwest to northeast seems to define the geometry of the foreland basin **(Fig. 7.2** & **7.3)**. It appears that overall foreland basin geometry of the Ganga basin is controlled by flexure subsidence related to evolution of adjacent Himalaya orogen (Burbank et al., 1996). The distributions of hypocenters of events have brought out a basin like structure of the crust below the IGP. The depocenter of sedimentary structure above the activity located close to the front of the collision belt near the MFT and MBT. Because of this sediment pinch–out and migration outwards due to the motion along thrust wedge (Huyghe et al., 2001 and Mugnier and Huyghe, 2006). From the distribution of earthquakes between the MFT and the MBT, the fault bend fold model is postulated (Yeats & Thakur, 1998). This model represents folded structures of anticlines and synclines. The MFT is represented by fault propagation folds and marks the southern edge of the basal flat and overriding ramp (Suppe and Medwedeff,

1990). In the northern part up to the Srinagar thrust (SNT) a ramp like structure forming sequence of imbricate thrusts overrides the basal flat. The space-depth distribution of local seismicity is shown on the tectonic model given by Mugnier and Huyghe, (2006) for IGP. Based on this distribution the proposed model is given in **Fig. 7.3.**

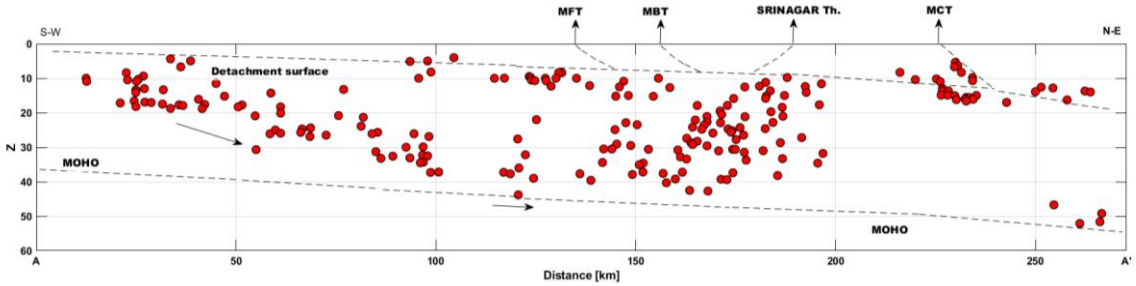

Fig. 7.2 Depth distribution of seismic activity along traverse A-A' as shown in **Fig. 7.1**.

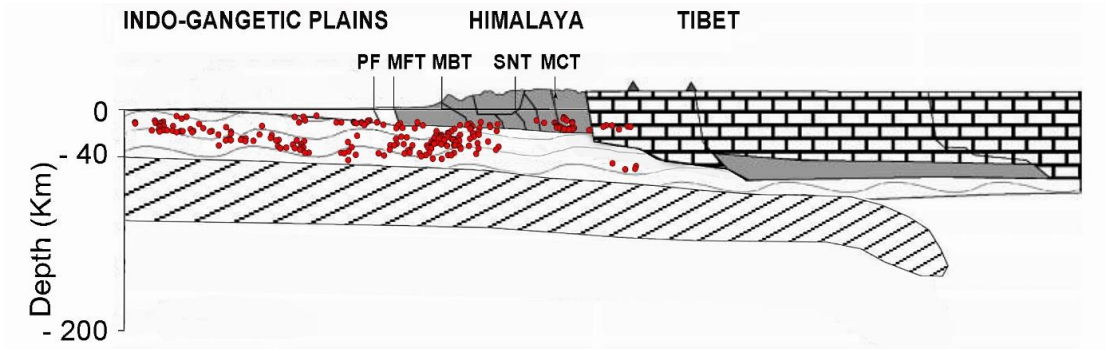

Fig. 7.3 Schematic sketch of proposed model of IGP, Himalaya and Tibet along with hypcentral distributions of 265 earthquakes (modified after Mugnier and Huyghe, 2006).

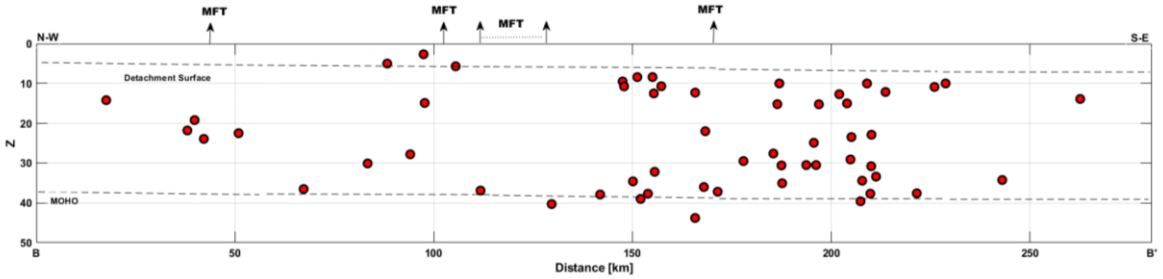

Fig. 7.4 Depth distribution of seismic activity along traverse B-B' as shown in **Fig. 7.1**.

The depth section B-B' depicts the seismic activity along a 280-km-long northwest-southeast trending segment of the MFT. Because of the local variation in the strike direction of the MFT, the traverse A-B cuts the surface trace of the MFT at several locations (**Fig. 7.1**). Broadly speaking the MFT is a northwest-southeast striking tectonic boundary thrust that seems to dip in the northeast direction. The depth distribution of seismic activity have brought out that events either occur at vary shallow depths (< 10 km) or at depths between 30 and 40 km (**Fig. 7.4**). Some of the events at shallow depths (seven events) occurred to the south of the MFT and their locations coincides with the Piedmont fault which trends northwest-southeast and is located at a distance of 30 km west of Roorkee with a gentle dip of 6^0 -7^0 due northeast (Thakur, 2013). Along this traverse the depths of the events found to decrease from northwest to southeast. Further, the

seismic activity exhibits a distinct pattern in the depth distribution as majority of the events occurs either at depths from 30 to 40 km or at shallow depths between about 8 and 10 km. The region between 10 and 50 km show increasing focal depth as we move further away from Mahendragarh-Dehradun Sub-Surface Fault (MMDS). The local events at shallow depths seem to represent the seismic activity of the upper parts of the MHT, in the vicinity of the MFT and the Piedmont fault zone. It appears that the depth of the upper surface of the Indian plate in the vicinity of MFT is about 10 km. This depth is in agreement with the depth estimated by other investigators (Khattri et al., 1989; Kanaujia et al., 2015; 2016). Based on the occurrence of events at a deeper level, the likely depth of the Moho discontinuity is at about 40-50 km. It has been postulated that the 1905 Kangra earthquake source zone lies beneath the MFT, and could be at a depth of 30-40 km (Bhattacharaya and Kayal, 2005). The occurrences of local events at deeper level lend support to this hypothesis that the source zones of great earthquakes may be located at the Moho depth. However, this does not agree with the tectonic model of Seeber et al. (1981) that the great Himalayan earthquakes occur because of rupturing of the upper surface of the Indian plate which is at a depth of about 10 km.

8. Conclusions

The objective of this study is to understand the seismotectonics of the region around IGP and the Garhwal Sub Himalaya. The main emphasis is to study the contemporary local seismicity of the segment of Main Frontal Thrust (MFT) also called as the Himalayan Frontal Thrust (HFT). From the analysis and interpretation of local earthquake data collected from the region the space-depth distributions of seismicity, mechanics of the faulting and stress orientations have been studied. The major findings are as follows:

The FPSs encompass three tectonic domains reveled tectonic deformations of thrust, normal and strike–slip type. Seismic activity at shallow depths in the vicinity of the HFT seems to overlap the Piedmont fault which clustered 20 km west of Roorkee in the northwest-southeast direction, with a gentle dip of 6^0 -7^0 due north-east and showing acute angle dip at NW direction. This activity at shallow depths located adjacent to the MFT and Piedmont fault, indicate normal faulting. The normal faulting in IGP is attributed to lithospheric flexing due to bending of Indian plate and subsequently stretching at frontal part of IGP and forming of the peripheral foreland basin at later part. The activity that occurs to the south of the study area at a distance of about 100 km from MFT showed mostly thrust faulting. Part of the activity that occurs to the northeast of MFT follows the trend of Ganga river and seems to be related to Ganga tear fault. Activity aligned parallel to the MDF showed strike-slip mechanisms with lower focal depths. The inversion results of FPSs of 69 events suggest a dominant reverse faulting with a strike slip component on a preferred north-dipping plane. The maximum principal stress is oriented in N45°E with a 12° plunge. This direction of maximum principal stress largely agrees with the direction of northward movement of the Indian plate. The depth wise stress inversion results also show that the direction of compressive stress is near NNE-SSW in the IGP. The normal faulting in IGP is attributed to lithospheric flexing due to bending of Indian plate and causes the genesis of peripheral foreland basin.

In the present study, the proposed depth of the upper surface of the Indian plate in the IGP (southwest of the MBT) is about 8-10 km. Earthquake on other hand, also show a much deeper seismogenic source zone (depth 30-40 km) in the vicinity of HFT. It seems that, stress is accumulated in the lower crust of the under-thrusting Indian plate at a depth of 30-40 km much below the plane of detachment. From the pattern of space-depth distribution of seismicity, a major tectonic feature has been delineated to the southwest of the MFT, at least up to the depth of 30 km. The focal depths of events increase from 10 km to 30 km as we traverse from southwest to northeast. This shows a seismogenic feature with linear dimension of about 80 km. This hidden seismogenic feature beneath the IGP continues from upper crust to lower crust.

11. Acknowledgement

Authors acknowledge with thanks the Tehri Hydro-Development Corporation India Ltd. (THDCIL), Rishikesh for sponsoring the deployment and operation of 12-station Seismological Network around Tehri region that provided the local earthquake data used in the present study.

12. References

[1] Bhattacharya, S. N. and J. R. Kayal (2005), Seismicity of the Himachal Himalaya: constraint from local seismic network, *Geo Survey Ind Special Publication* 85, 71-79.
[2] Burbank, D.W. (1996), *Richard A. Beck, and Thomas Mulder*, 9 The Himalayan foreland basin.
[3] Gephart, J. W. (1990), FMSI: A FORTRAN program for inverting fault/slickenside and earthquake focal mechanism data to obtain the regional stress tensor, *Computers & Geosciences*, 16(7), 953-989.
[4] Gephart, J. W. and D. W. Forsyth (1984), An improved method for determining the regional stress tensor using earthquake focal mechanism data: application to the San Fernando earthquake sequence, *Journal of Geophysical Research: Solid Earth* (1978–2012), 89 (B11), 9305-9320.
[5] Gillard, D., M. Wyss, and J. S. Nakata (1992), A seismotectonic model for western Hawaii based on stress tensor inversion from fault plane solutions. *Journal of Geophysical Research: Solid Earth*, *97*(B5), 6629-6641.
[6] Hough, S. E., Bilham, R., Ambraseys, N., and Feldl, N. (2005). The 1905 Kangra and Dehra Dun earthquakes. *Geol. Surv. India, Spec. Publ*, 85, 15-22.
[7] Huyghe, P., Galy, A., Mugnier, J. L., and France-Lanord, C. (2001), Propagation of the thrust system and erosion in the Lesser Himalaya: Geochemical and sedimentological evidence. *Geology*, 29(11), 1007-1010.
[8] Kanaujia, J., Kumar, A., and Gupta, S.C. (2015), 1D velocity structure and characteristics of contemporary local seismicity around the Tehri Region, Garhwal Himalaya. *Bulletin of the Seismological Society of America*. *105*(4), 1852–1869.
[9] Kanaujia, J., Kumar, A., and Gupta, S.C. (2016), Three-dimensional velocity structure around the Tehri region of the Garhwal Lesser Himalaya: constraints on geometry of the underthrusting Indian plate. *Geophys. J. Int.*, 2*05*(4), 900–914.
[10] Kayal, J. R. (2010), Himalayan tectonic model and the great earthquakes: An appraisal, Geomatics, Natural Hazards and Risk, 1.1, 51-67.
[11] Khattri, K. N., Chander, R., Gaur, V. K., and Sarkar, I. (1989). New seismological results on the tectonics of the Garhwal Himalaya. *Proceedings of the Indian Academy of Sciences-Earth and Planetary Sciences*, 98(1), 91-109.
[12] Kumar, A., A. D. Pandey, M. L. Sharma, S. C. Gupta, A. K. Verma, and B. K. Gupta (1994), Processing and preliminary interpretation of digital data obtained from digital seismic array in Garhwal Himalaya, *Proc.10th Symposium on Earthquake Engineering, University of Roorkee, Roorkee, India*, 16–18 November 1994, Vol. 1, 141–152.
[13] Lienert, B.R. and J. Havskov (1995), A computer program for locating earthquakes both locally and globally, *Seismological Research Letters*, 66.5, 26-36.
[14] Mahesh, P., S. Gupta, U. Saikia and S.S. Rai (2015), Seismotectonics and crustal stress field in the Kumaon–Garhwal Himalaya, *Tectonophysics*, 655, 124-138.
[15] Mugnier, J. L., and Huyghe, P. (2006). Ganges basin geometry records a pre-15 Ma isostatic rebound of Himalaya. *Geology*, 34(6), 445-448.
[16] Sen, A. (2016), Seismotectonics of Main Frontal Thrust and Indo-Gangetic Plains around Roorkee., Ph.D. Thesis, IIT Roorkee, pp 1-192.
[17] Sen**,** A.**,** S.C. Gupta, Ashwani Kumar, M.L. Sharma (2018), Local tectonic stress field in the environs of Main Frontal Thrust and Ganga Foredeep in the Garhwal Hiamalaya and its seismotectonic implications, Proc. of *16th Symp. on Earthquake Engg*., December 20-22, 2018, IIT Roorkee, Paper No. 134.
[18] Seeber, L., Armbruster, J. G., and Quittmeyer, R. C. (1981), Seismicity and continental subduction in the Himalayan arc. Zagros Hindu Kush Himalaya Geodynamic Evolution, 215-242.
[19] Sharma, M.L. and C. Lindolhm (2012), Earthquake hazard assessment for Dehradun, Uttarakhand, India, including a characteristic earthquake recurrence model for the Himalaya Frontal Fault (HFF), *Pure and Applied Geophysics*, Vol. 169, pp. 1601–1617.
[20] Sharma, M. L., Gupta, S. C., Jindal, A. K., Jain, S. K., Arup Sen (2016), Local Seismological Network around Tehri Dam, *THDC Hydro Tech, Volume 4, issue II*, 32-39, THDC
[21] Snoke, J. A., J. W. Munsey, A.C. Teague and G.A. Bollinger (1984), A program for focal mechanism determination by combined use of polarity and SV- P amplitude ratio data, *Earthquake Notes*, 55, 3-15.
[22] Suppe, J., and Medwedeff, D. A. (1990). Geometry and kinematics of fault-propagation folding. *Eclogae Geologicae Helvetiae*, 83(3), 409-454.
[23] Thakur, V.C. (2013), Active tectonics of Himalayan frontal fault system, *International Journal of Earth Sciences*, 102(7), 1791-1810.
[24] Yeats, R. S., and Thakur, V. C. (1998). Reassessment of earthquake hazard based on a fault-bend fold model of the Himalayan plate-boundary fault. *Current Science*, 74(3), 230-233.

